

PIOTR HOLNICKI*, ANTONI ŻOCHOWSKI*,
ALEKSANDER WARCHAŁOWSKI**

REGIONAL-SCALE AIR POLLUTION DISPERSION MODEL REGFOR1***

In the paper, an implementation of a single-layer dynamic model for SO_x air pollution forecasting on regional scale is presented. The computation method simulates the transport of the primary and the secondary pollutants following the wind trajectories. The model equations take into account transport, deposition (dry and wet) and chemical transformation processes.

The model is designed for evaluation of the environmental impact of major emission sources and, eventually, for emission control. The main output consists of the set of unit concentration maps for selected, individual sources, corresponding to the unit emission intensity. The assumed linearity of the dispersion process allows us to treat each source individually, and then to compute the total concentration map as a superposition of the individual contributions. The test computations have been performed for the set of major power plants in Poland.

1. THE TRANSPORT MODEL FORMULATION

The model presented in the paper is aimed at computing short-term forecasts of air pollution related to specified emission sources, evaluating contribution of each source in the resulting pollution field and, ultimately, utilizing those data in air quality control. The basic output of the model has a form of 24-hour forecast of the total SO₂ concentration in the domain or the form of individual maps representing contribution of each emission source. Such a map characterizes environmental impact of a specified source.

Calculation of the transport of sulphur pollution is carried out by Lagrangian-type, single layer trajectory model. It allows calculation of the concentrations averaged over the mixing layer. The mass balance for the pollutants is calculated for air parcels following the wind trajectories. The model is source-oriented, and the trajectory that

* Systems Research Institute, Polish Academy of Sciences, Warsaw, Poland.

** Warsaw University of Technology, Institute of Environmental Engineering Systems, Warsaw, Poland.

*** Constructed partially in the framework of ESPRIT Project 20288 Cooperation Research in Information Technology (CRIT2): *Evolutionary Real-Time Optimization System for Ecological Power Control*.

starts at the specific emission source is observed until the mass of the parcel drops below 1% if its initial value or the parcel leaves the computational area. The technique is in turn applied to all the individual sources, giving the unit *transfer matrices* as a result. Multiplying these matrices by the real emissions and summing over the set of all the sources under consideration give the total concentration map.

The model takes into account two basic polluting components, SO_2 and SO_4^{2-} . The uniform space discretization step, $h = \Delta x = \Delta y = 10$ km is applied in the computational algorithm. Points along the trajectory are determined at discrete time moments based on the interval $\tau = 15$ min. The main output constitutes the concentrations of SO_2 averaged over the discretization element and the mixing layer height. Based on the total mass of the "packet" of the pollutant emitted over the interval τ the initial concentrations are calculated according to the formulae

$$q_1 = \frac{(1 - \beta)E\tau}{HM \cdot h^2}, \quad (1)$$

$$q_2 = \frac{\beta E\tau}{HM \cdot h^2}, \quad (2)$$

where: q_1, q_2 denote the concentrations of SO_2 and SO_4^{2-} [$\mu\text{g}/\text{m}^3$], E [$\mu\text{g}/\text{s}$] is the total sulphur emission, β – the fraction emitted directly as SO_4^{2-} , HM [m] – the mixing layer height.

The continuity equations for both components reflect the spatial and temporal transformations of their initial values. They included transport, chemical transformations $\text{SO}_2 \Rightarrow \text{SO}_4^{2-}$, dry deposition, scavenging by precipitation and have a form

$$\frac{\partial q_1}{\partial t} + \mathbf{w} \nabla q_1 + (k_{d_1} + k_{w_1})q_1 + k_t q_1 = 0, \quad (3)$$

$$\frac{\partial q_2}{\partial t} + \mathbf{w} \nabla q_2 + (k_{d_2} + k_{w_2})q_2 = k_t q_1, \quad (4)$$

where: k_{d_i} – dry deposition coefficient [1/s], k_{w_i} – coefficient of wet deposition due to scavenging by precipitation [1/s], k_t – coefficient of chemical transformation of $\text{SO}_2 \Rightarrow \text{SO}_4^{2-}$ [1/s], $\mathbf{w} = [u, v]$ – wind velocity vector [m/s]. The emission term does not appear on the right-hand side of (3) and (4), since the model simulates dispersion and environmental impact (spatial and temporal) of the initial concentrations (1) and (2) related to a source.

If all the coefficients in (3), (4) are assumed constant over the interval $[t, t + \tau]$, the solutions can be expressed [2] in the following form

$$q_1(t + \tau) = q_1(t) \exp(-(k_{d_1} + k_{w_1} + k_l))\tau, \quad (5)$$

$$q_2(t + \tau) = \frac{k_l q_1(t)}{k_{d_2} + k_{w_2}} [1 - \exp(-(k_{d_2} + k_{w_2})\tau)] + q_2(t) \exp(-(k_{d_2} + k_{w_2})\tau). \quad (6)$$

The coefficients, which represent the decline due to dry deposition in (3)–(6), are defined as follows:

$$k_{d_i} = \frac{v_{d_i}}{HM}, \quad (i = 1, 2), \quad (7)$$

where dry deposition velocity for SO_2 – v_{d_1} [m/s] is preprocessed by a specialized algorithm developed at RIVM (the Netherlands) [4]–[6] and modified in the Institute of Environmental Engineering Systems (Warsaw Institute of Technology). Land-use characteristics utilized in this model are based on [7]. Moreover, basing on the approach presented in [2], the dry deposition velocity for SO_4^{2-} is assumed $v_{d_2} = 0.2 v_{d_1}$.

Wet deposition depends on precipitation intensity and is expressed, in general, as

$$k_{w_i} = \frac{A_i P}{HM}, \quad (i = 1, 2), \quad (8)$$

where P denotes the precipitation height in [mm] accumulated over the time interval. Basing on [2], the scavenging factor for SO_2 reflects the seasonal fluctuations in air temperature, and is parameterized as follows

$$A_1 = 3 \cdot 10^5 + 1 \cdot 10^5 \sin[2\pi(T - T_0)/T_a]. \quad (9)$$

T is the current day of the year, $T_0 = 80$ days, and $T_a = 365$ days. For simplicity, the scavenging factor for SO_4^{2-} is assumed constant (compare [2]),

$$A_2 = 1 \cdot 10^6. \quad (10)$$

In analogous way, the chemical transformation coefficient in (3)–(6) can be defined according to the formula

$$k_l = a_l + b_l \sin[2\pi(T - T_0)/T_a], \quad (11)$$

where the parameters a_l , b_l are constant,

$$a_l = 3 \cdot 10^{-6} [1/s], \quad b_l = 2 \cdot 10^{-6} [1/s],$$

while T , T_0 and T_a are defined as in (9).

The main output generated by the model is a set of the unit *transfer matrices* for all the emission sources considered. The respective output matrix relates the respective SO_2 and SO_4^{2-} concentration forecasts to the unit emission intensity of the source. Assuming linearity of the dispersion process, we can compute the total concentration map as a superposition of contributions of the individual sources.

The pollution forecast calculated by the model relates to the 24-hours time interval. However, the current concentration of a pollutant at any receptor site also depends on the previous releases from other sources. The latter pollutants are transported and transformed, depending on the wind-field and other meteorological conditions. Ultimately, they form the background concentration field for the forecast.

In order to take the previous pollution into account, it is assumed here that the influence of the released pollutants may be neglected after 3 days. Thus, the model allows us to calculate dispersion and transformations of the pollutants over the computational area, starting from 48 hours before the beginning of the forecast period. The contribution of these pollutants is taken into account only over that period (the last 24 h). The sum of the contributions of all the sources, taken with their real emission in the past two days, constitutes the background concentration of the forecast.

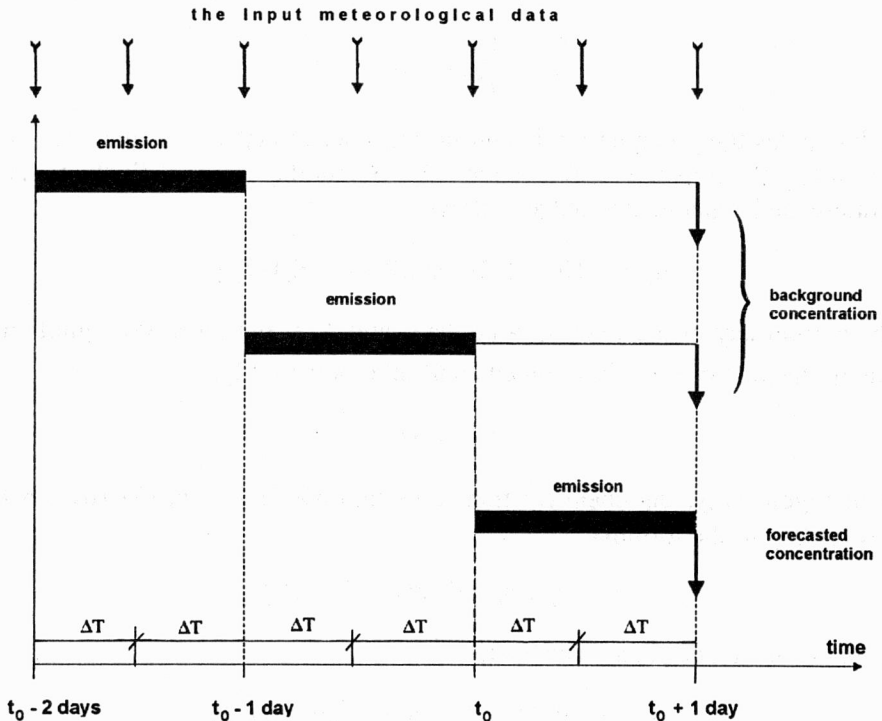


Fig. 1. The diagram of the forecast and background concentration computing

Figure 1 explains the algorithm of calculation of the basic forecast and background concentration maps. Let us denote by t_0 the initial time of the current 24-hour forecast, and assume that the basic time interval for the input data is $\Delta T = 2$ h. Then, the sequence of the input data for the interval $\langle t_0, t_0 + 2\Delta T \rangle$ is used for generating the forecast of the concentration map at $t_0 + 2\Delta T$. In the same way, the respective sequence of the input data from two previous time intervals, namely $\langle t_0 - 4\Delta T, t_0 - 2\Delta T \rangle$ and $\langle t_0 - 2\Delta T, t_0 \rangle$, is utilized for generating the background map for the same time moment.

The algorithm of generating the unit pollution maps consists of several steps and is repeated for all the sources under consideration. It consists of the following steps:

- reading the set of the input data,
- interpolating meteorological data in space and time,
- generating the wind trajectory for the period of the forecast,
- calculating the transport of the package along the trajectory,
- calculating the physical and chemical transformations,
- calculating the resulting concentration field.

The forecast contribution of a source to the resulting concentration field is calculated by the multiplication of the respective unit concentration map by the predictor (or the actual) emission intensity of this source. The resulting concentration map is then obtained as the superposition of the individual contributions.

In a similar way, the background pollution map is computed according to the diagram shown in figure 1, but the total emission field represents in this case the real emissions of the sources in the previous time intervals, i.e. $\langle t_0 - 4\Delta T, t_0 - 2\Delta T \rangle$ and $\langle t_0 - 2\Delta T, t_0 \rangle$.

2. THE WIND FIELD SUBMODEL

One of the basic meteorological inputs of the pollution transport model is the wind field prediction within the time of the forecast. Due to the structure of the transport model, the wind field should be a single-layer approximation of the three-dimensional field, averaged over the mixing layer HM . The implementation has been worked out for the rectangle area of $900 \text{ km} \times 750 \text{ km}$ shown in figure 2 in the EMEP coordinates. The uniform space discretization step, $h = \Delta x = \Delta y = 10 \text{ km}$, was applied in the computational algorithm.

The wind trajectories for the region discussed here are preprocessed basing on the data from four aerological stations shown in figure 2. The trajectory generation procedures uses the following input data: (i) a complete set of wind field measurements in the selected field stations, (ii) the coordinates of emission source location. The approach applied is based on the spatial and temporal interpolation of the sequence of

meteorological data obtained from the selected measurement stations. Each station records the set of data twice a day; the respective time interval is $\Delta T = 12$ h. The set of measurement data contains the following wind characteristics:

- components of the anemometric wind, u_A, v_A ;
- components of the geostrophic wind (850 hPa), u_G, v_G .

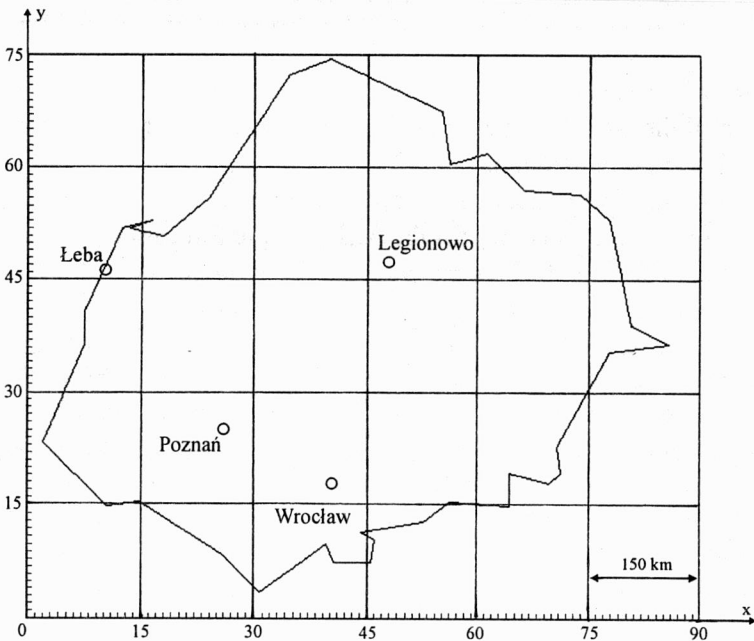


Fig. 2. Region in EMEP coordinates and aerological measurement station

The above data have to be interpolated in space and time over the computational domain. The resulting wind field, averaged over the mixing layer, should also reflect some additional constraints. One of them, imposed due to the general model of atmospheric circulation, is the continuity condition of the following form:

$$\frac{\partial u}{\partial x} + \frac{\partial v}{\partial y} = 0. \quad (12)$$

The field is preprocessed by the spatial interpolation of the measured input data and time interpolation of the consecutive episodes. The approach applied in the interpolation algorithm is based on the assumption that the movement of the atmosphere has the rotational character – it rotates about certain centers located in regions of high or low pressure. The wind components in such a field satisfy the following relation:

$$[u(x, y), v(x, y)] = k \cdot [-(y - y_0), (x - x_0)], \quad (13)$$

where the point (x_0, y_0) denotes the center of the vortex.

The trajectory is evaluated for an individual package of pollutant emitted by a source. Denoting by (x_p, y_p) the coordinates of the current position of a pollutant package, the equations of its trajectory have the form

$$\frac{dx_p}{dt} = u(x_p, y_p, t), \quad x_p(0) = x_0; \quad \frac{dy_p}{dt} = v(x_p, y_p, t), \quad y_p(0) = y_0, \quad (14)$$

where (x_0, y_0) is the initial position of the package.

The solution algorithm is based on a simple finite-difference approximation. For the time discretization step τ , one obtains

$$\begin{aligned} x_p((k+1)\tau) &= x_p(k\tau) + \tau u(x_p(k\tau), y_p(k\tau), k\tau), \\ y_p((k+1)\tau) &= y_p(k\tau) + \tau v(x_p(k\tau), y_p(k\tau), k\tau). \end{aligned} \quad (15)$$

Since the values of the wind velocity components u and v are measured every 12 hours, the time interval ΔT has to be additionally discretized for computational purposes. Therefore, two time scales are applied

- the division of the forecast horizon (e.g. one year) into N 12-hour intervals ΔT ,
- the division of each interval ΔT into m time-steps of the length τ , i.e. $\Delta T = m\tau$.

Thus, the total period of the forecast is $T_N = m \cdot N \cdot \tau$. At the end of each time interval $(i\Delta T, (i+1)\Delta T)$ we know the wind measurements in meteorological stations. For the moment $t_{i,j} = i\Delta T + j\tau$, ($j < m$), we must perform the interpolation of the wind vector $\mathbf{w} = [u, v]$ between two consecutive values: $\mathbf{w}(i\Delta T)$ and $\mathbf{w}((i+1)\Delta T)$.

Given the values of the wind vector at every time moment at the measuring stations, the wind components at any selected point of the computational domain are calculated by means of the interpolation procedure described by the above formulae (13)–(15). As a result we obtain the trajectory of the pollutant package up to the moment when it leaves the computational area, or vanishes (the total mass of the package drops below 1% of its initial value) due to chemical transformations or deposition process.

The effective stack height is calculated according to the Holland formula (Lyons and Scott, 1990), and the initial development of the pollutant package is parameterized by an artificial shift of the emission source coordinates.

3. THE TEST APPLICATION

The model has been applied to generating 24-h forecast of SO_2 concentration for the major power and heating plants of the Polish energy sector. The computational

domain is an EMEP-oriented rectangle of 900×750 km containing Poland. The uniform resolution based on the grid element of $10 \text{ km} \times 10 \text{ km}$ is applied, thus the size of the grid considered is 90×75 .

Calculations were performed for the set of 91 main power plants of the Polish energy sector (the dominant sources are shown in the table in an aggregated form). The position of each source in the table is shown in coordinates of the discrete domain. The last two columns on the table represent emission quantities averaged over the winter and summer seasons, respectively. The simulation was performed for 2 selected meteorological episodes of the winter season of 1999 and one episode of the summer season of the same year. Each episode consists of several consecutive days and is represented by a sequence of the respective meteorological input data and the intensity of emission sources.

Table

Aggregated emission inventories of the major sources (data for the year 1996)

No.	Power plant	Numb. of stack	Grid element (x,y)-coord.	Range of stacks' heights [m]	SO ₂ emission – winter [Mg h ⁻¹]	SO ₂ emission – summer [Mg h ⁻¹]
1	Adamów	2	(31.6, 5.6)	150	1.9424	1.0251
2	Bełchatów	3	(48.2, 32.1)	300	30.7043	19.8995
3	Bydgoszcz	3	(27.4, 38.8)	73–100	3.3046	0.4915
4	Chorzów	2	(40.5, 18.4)	100–180	1.6023	0.1940
5	Dolna Odra	2	(9.7, 22.1)	250	9.4608	4.9932
6	Gdańsk	3	(45.8, 36.2)	120–200	2.8193	0.3845
7	Gdynia	2	(45.6, 36.6)	85–150	1.9769	0.4185
8	Jaworzno	2	(58.7, 24.7)	120–300	5.7122	3.2146
9	Konin	4	(31.6, 5.6)	100–120	4.6431	2.9376
10	Kozienice	3	(55.7, 47.4)	200–300	8.5628	4.5192
11	Kraków	2	(63.8, 27.0)	225–260	4.5560	0.9257
12	Łagisza	2	(57.5, 24.7)	160–200	4.7152	2.4885
13	Łaziska	2	(57.7, 21.0)	160–200	5.4685	3.0322
14	Łódź	6	(42.6, 57.9)	50–200	8.4557	1.3328
15	Ostrołęka	2	(42.6, 57.8)	120–250	4.7678	2.0003
16	Pątnów	2	(35.5, 34.0)	150	15.6949	9.3085
17	Połaniec	2	(66.2, 38.3)	250	12.1660	6.4210
18	Rybnik	2	(55.7, 19.5)	260–300	8.3418	4.4112
19	Siekierki	2	(48.8, 49.0)	120–200	6.8124	1.0926
20	Siersza	2	(60.3, 25.3)	150–260	3.8595	2.0369
21	Skawina	2	(63.6, 25.7)	120	3.2744	1.7281
22	Turów	3	(31.6, 5.6)	150	17.8486	10.3945
23	Wrocław	2	(40.5, 18.4)	120–180	3.6988	0.5794
24	Zabrze	2	(40.5, 18.4)	100–180	2.2615	0.3868
25	Żerań	3	(47.6, 49.2)	100–200	3.2003	0.4876

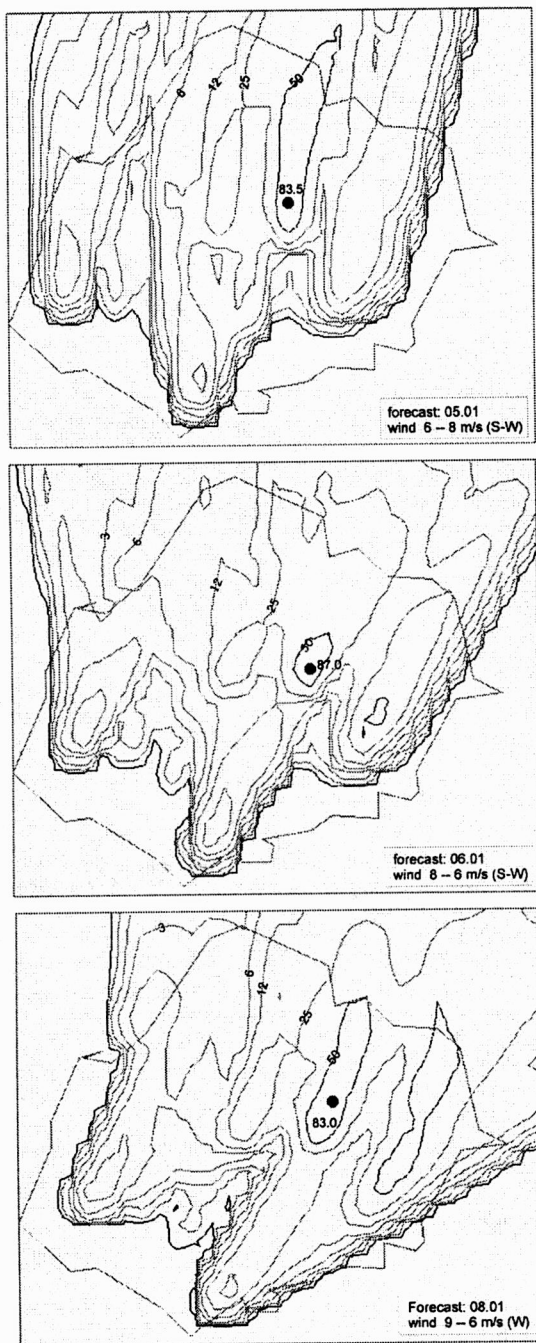


Fig. 3. Short-term forecast of SO₂ [$\mu\text{g}/\text{m}^3$] concentration for the winter-season – episode 05.01– 08.01.99

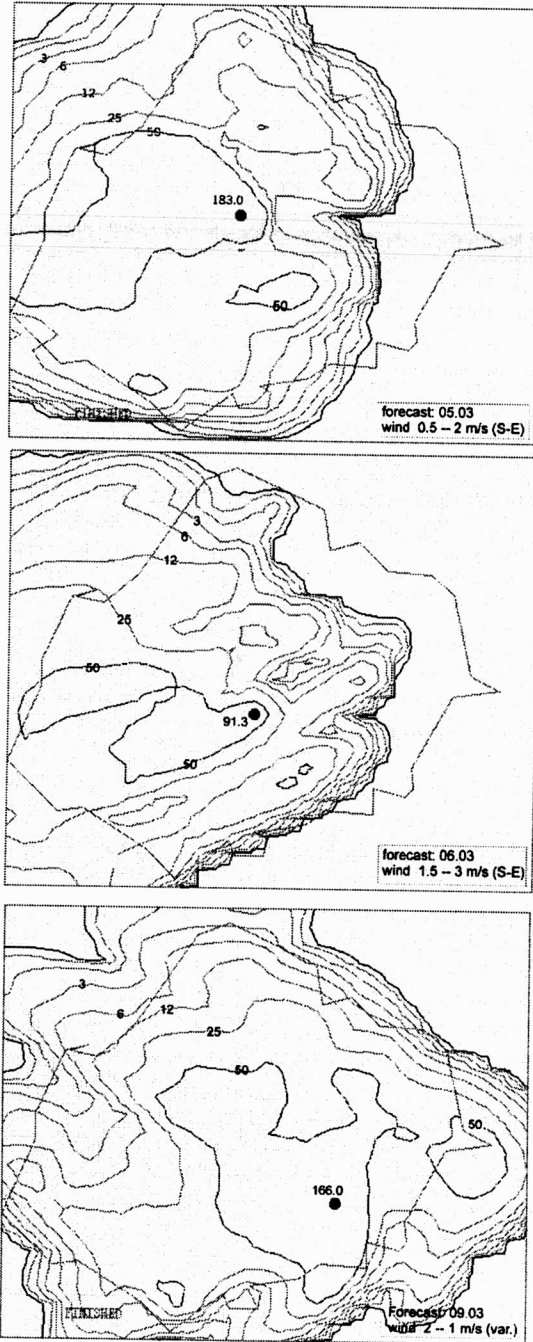


Fig. 4. Short-term forecast of SO₂ [$\mu\text{g}/\text{m}^3$] concentration for the winter-season – episode 05.03– 09.03.99

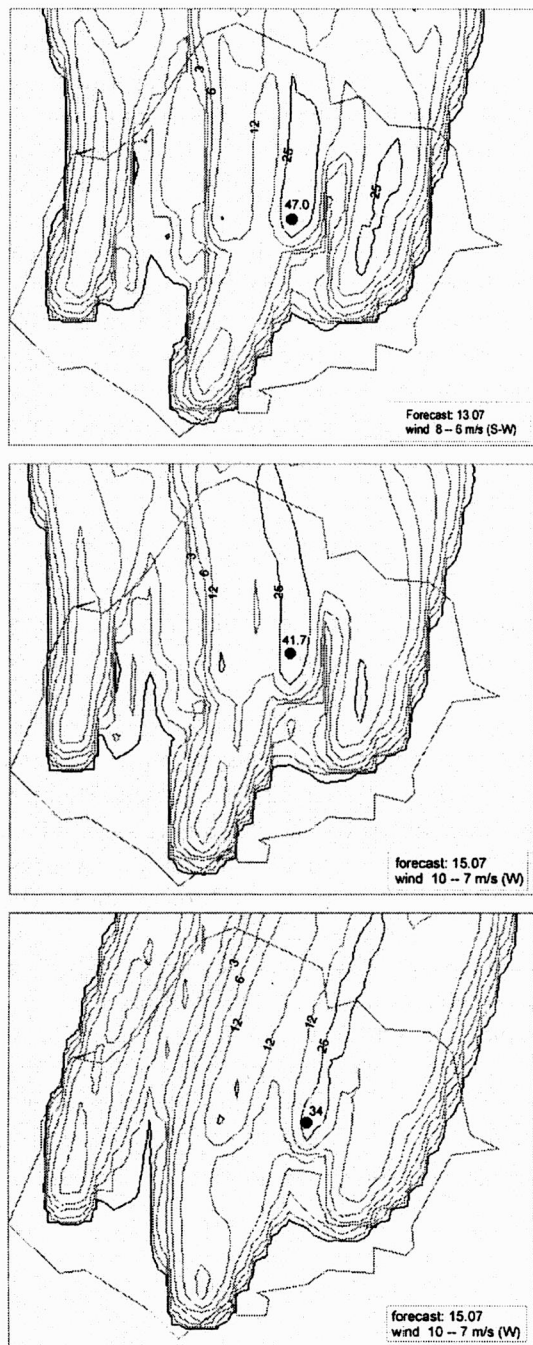


Fig. 5. Short-term forecast of SO₂ [$\mu\text{g}/\text{m}^3$] concentration for the summer-season – episode 13.07–15.07.99

The results of computation are shown in figures 3–5. They present the field of total SO₂ concentration for three selected days of each meteorological episode. Based on the algorithm described in the previous sections, each map is calculated according to the following steps: i) generating the set of the unit concentration matrices for a given meteorological scenario, ii) generating the background concentration map based on the actual SO₂ released and meteorological data of the previous two days, iii) calculating the total concentration forecast as a superposition of the background map and the sum of the contributions of all the sources (the concentration represented by a unit map multiplied by real emission, see the table).

The area of the maximum concentration is related to Bełchatów power plant as well as power plants located in Upper Silesia Region. The maximum values strongly depend on the meteorological conditions, mainly on the wind velocity. It can be seen in figure 3 and figure 4 that very high concentration episodes relate to week and variable wind conditions when the cumulation of pollution may occur.

4. CONCLUSIONS

The model discussed in the paper is an implementation of a Lagrangian-type, dynamic algorithm. Mathematical description includes the basic factors (meteorological, chemical and the others) that determine dispersion process of air pollutants. An essential part of the model constitutes the built-in wind preprocessor, which generates the wind field prediction in the computational area, including its spatial and temporal evolution within the forecast interval. The respective set of the measurement data is essential for this process.

Computer implementation of the REGFOR1 algorithm has been worked out in the Fortran 90 code. It can be implemented both on PS's as well as on the Unix-based platforms. Computing time of 48-hour pollution forecast on PC (Pentium II processor) for the set of 91 sources takes 90 seconds.

The results presented in section 3 show that the model can be directly applied to short-term forecasting of air pollution. Generally, it can be utilized as a decision support tool in the area of regional planning focussed on environmental effects. Due to the dynamic character of the model and relatively short computing time related to the forecast generation, the real-time emission control is another field of possible applications. The task of this type was developed in the framework of the European ESPRIT Project 20288 (CRIT2), where REGFOR1 model was integrated with an optimal control algorithm and used in the power control process related to the Polish energy sector.

REFERENCES

- [1] VOLDNER E.C., BARRIE L.A., SIROIS A., *A literature review of dry deposition of oxides of sulphur and nitrogen with emphasis on long-range transport modeling in North America*, Atmospheric Environment, 1986, 20, 2101–2133.

- [2] SANDNES H., *Calculated budgets for airborne acidifying components in Europe*, EMEP/MSC-W, The Norwegian Meteorological Institute, Report 1/93, Blindern, July, 1993.
- [3] GOLDER D., *Relations among stability parameters in surface layer*, Boundary Layer Meteorology, 1972, 3, 47–58.
- [4] ERISMAN J.W., *Atmospheric deposition of acidifying compounds in the Netherlands*, PhD-thesis, 1992, University of Utrecht, the Netherlands.
- [5] ERISMAN J.W., Van PUL W.A.J., WYERS G.P., *Parameterization of surface resistance for the quantification of atmospheric deposition of acidifying pollutants and ozone*, Atmospheric Environment, 1994, 28, 16, 2595–2607.
- [6] Van PUL A., *Dry deposition model (FORTRAN code, DEPAC)*, Report LLO/RIVM, 1994, Bilthoven, the Netherlands.
- [7] Land-use source data, (ELU) European Land Use Database.
- [8] TROJANOWSKI K., *Evolutionary real-time optimization system for ecological power control – system documentation*, CRIT2 Technical Report, ICS PAS, Warsaw, 2000.

REGIONALNY MODEL ROZPRZESTRZENIANIA SIĘ ZANIECZYSZCZEŃ ATMOSFERYCZNYCH (REGFOR1)

Przedstawiono implementację jednowarstwowego modelu rozprzestrzeniania się zanieczyszczeń (tlenków siarki) w skali regionalnej. Opis matematyczny jest oparty na równaniach transportu, w których uwzględniono procesy depozycji oraz przemian chemicznych, w algorytmie obliczeniowym natomiast wykorzystano równania trajektorii pola wiatru.

Model umożliwia ilościową ocenę krótkoterminowego wpływu wybranych źródeł emisji na środowisko, a także sterowanie emisją. Podstawowe wyjście stanowią jednostkowe mapy przejścia emisja → stężenie charakteryzujące poszczególne źródła. Założona liniowość procesu dyspersji zanieczyszczeń pozwala obliczać sumaryczne pole ich stężenia jako superpozycję wpływu poszczególnych źródeł. Działanie modelu ilustrują wyniki obliczeń testowych, które wprowadzono dla grupy podstawowych obiektów energetycznych w Polsce.

